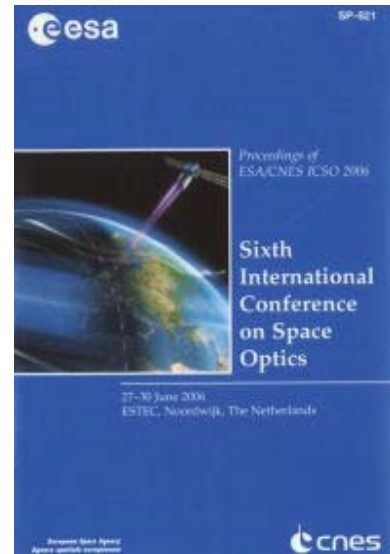


International Conference on Space Optics—ICSO 2006

Noordwijk, Netherlands

27–30 June 2006

Edited by Errico Armandillo, Josiane Costeraste, and Nikos Karafolas



Multi-axial interferometry: demonstration of deep nulling

*Christophe Buisset, Xavier Rejeaunier, Yves Rabbia,
Cyril Ruilier, et al.*



MULTI-AXIAL INTERFEROMETRY: DEMONSTRATION OF DEEP NULLING

Christophe Buisset^(1,2), Xavier Rejeaunier⁽¹⁾, Yves Rabbia⁽²⁾, Cyril Ruilier⁽¹⁾, Marc Barillot⁽¹⁾, Lars Lierstuen⁽³⁾, Josep Maria Perdigués Armengol⁽⁴⁾

(1) Alcatel Alenia Space, 100 Bd du midi, 06156 Cannes-la-Bocca Cedex, France,

Email: Xavier.Rejeaunier@alcatelaleniaspace.com

(2) Observatoire de la Côte d'Azur, Avenue Nicolas Copernic, 06130 Grasse, France,

Email: Christophe.Buisset@obs-azur.fr

(3) Kongsberg D & A, P.O. Box 26,N-2007 Kjeller or P.O. Box 1003 N-3601, Kongsberg, Norway,

Email: Lars.Lierstuen@kongsberg.com

(4) ESA-ESTEC, Postbus 299, 2200 AG Noordwijk, The Netherlands,

Email: Josep.Maria.Perdigués.Armengol@esa.int

ABSTRACT

The ESA-Darwin mission is devoted to direct detection and spectroscopic characterization of earth-like exoplanets. Starlight rejection is achieved by nulling interferometry from space so as to make detectable the faintly emitting planet in the neighborhood.

In that context, Alcatel Alenia Space has developed a nulling breadboard for ESA in order to demonstrate in laboratory conditions the rejection of an on-axis source. This device, the Multi Aperture Imaging Interferometer (MAII) demonstrated high rejection capability at a relevant level for exoplanets, in single-polarized and mono-chromatic conditions.

In this paper we report on the new multi-axial configuration of MAII and we summarize our late nulling results.

Keywords :

Exoplanets, Direct detection, Nulling interferometry, Polarization, Modal filtering, Darwin.

1. INTRODUCTION

The ESA-Darwin [1] and the NASA-TPF missions aim at direct detection and spectroscopic characterization of earth-like exoplanets. This objectives require to reduce the starlight at such a level that the faintly emitting planet becomes detectable (reduction by one million is the typical figure in the thermal infrared domain). In this context, nulling interferometry is one of the most promising instrumental approach. It is based on destructive interference for an on-axis star while keeping a constructive interference for the neighboring planet. The associated performance is quantified by the so-called rejection (ratio $R = \text{collected flux} / \text{residual flux}$), or equivalently by the inverse of this ratio, $N = 1/R$ called nulling depth (or simply nulling).

In its preparation to nulling missions, Alcatel Alenia Space has been developing for ESA the nulling interferometer MAII, a test bench² dedicated not only to demonstrate high (and stable) rejection but also to test various subsystems in order to explore and/or to Optimize various instrumental options, regarding both the set-up configuration and the components. The overall design of the bench was presented in 2004 by Weber & al. [2],[3]. At this time, the combination of the beams was co-axial and done via an Integrated Optic Beam Combiner (IOBC). Monochromatic and single-polarization nulling ratio $N = 10^5$ in the line with the needs of the missions have been obtained and thus demonstrated the efficiency of integrated optic components.

In 2004, ESA [4] proposed a novel combination scheme for a nulling interferometer: multi-axial single mode beam combining. It consists of coupling the output fields of a nulling interferometer into an unique single mode fibre which acts as modal filter and combiner. The principle of this combination scheme in the case of a 2-beams interferometer is shown in figure 1.

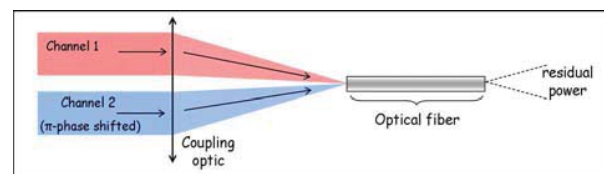


Fig. 1: Multi-axial beam combination principle.

In this context, Alcatel Alenia Space (AAS) upgraded MAII with the support of ESA so as to test multi-axial beam combination. From the paper written by Haguenaer & Serabyn [5] in 2006, we know that a similar approach was initiated in parallel at JPL.

In a section 2 we present the MAII testbed. In section 3 we present the nulling results obtained with the

multi-axial single-mode combination. In section 4 we discuss these results.

2. MAII OPTICAL DESIGN

The MAII breadboard is shown in figure 2. The main functions are: the star simulator, the amplitude matching device, the Optical Delay Lines (ODL), the Achromatic Phase shifter (APS) and the recombination part (co-axial or multi-axial).

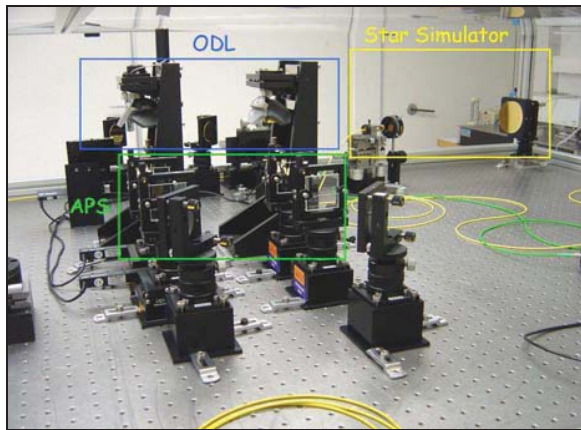


Fig. 2: MAII breadboard.

Figure 3 shows the multi-axial optical design of MAII.

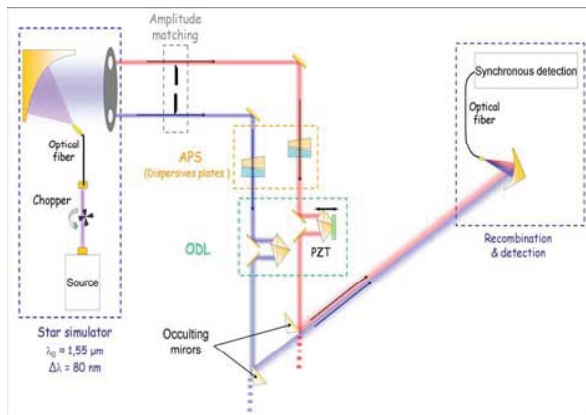


Fig. 3: Multi-axial design of MAII.

2.1.1. Star simulator

Figure 4 shows the star simulator of MAII. The ASE source is a polychromatic ($\lambda_0=1,55 \mu\text{m}$, $\Delta\lambda/\lambda \approx 5 \%$) and non-polarized.

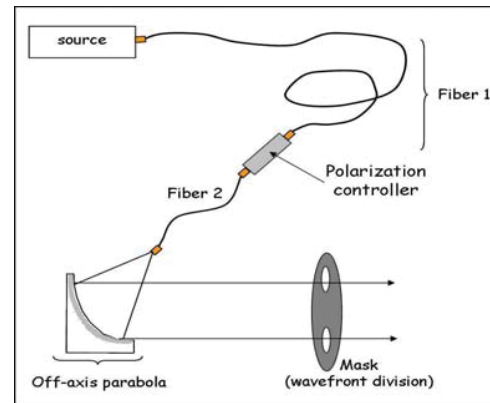


Fig. 4: Star simulator of MAII.

Following the source two fibres linked together via a polarization controller direct the light to a collimator (off-axis parabola) the simulated star being the exit end of fibre 2. A polarizer can be set inside the star simulator to work in single-polarization regime. Following the collimator, a mask produces two beams by wavefront division.

2.1.2. Amplitude matching device

Knife edges are translated inside the beams so as to achieve amplitude matching for the two interfering waves. With the use of translation stage, relative flux difference between the beams is better than 10^{-3} .

2.1.3. Optical Path Difference (OPD) adjustment and π phase shifting

Identical Optical Delay Lines (ODL) are installed along each arm of the interferometer. These ODL are equipped with a corner cube. OPD adjustment to zero is achieved by translating the corner cube by means of either translation stage (long stroke) or piezoelectric (high accuracy). During measurements, OPD is maintained adjusted manually. On the other arm, a similar static delay line keeps the symmetry of the interferometer.

2.1.4. Achromatic Phase shifter (APS)

The APS is composed of 2 wedged dispersive plates of different materials installed along each arm of the interferometer. A convenient combination of the plates thickness and an extra fine-tuning of the ODL yields the achromatic π phase shifting.

2.1.5. Multi-axial combination scheme

The multi-axial combination used in MAII is shown in figure 5.

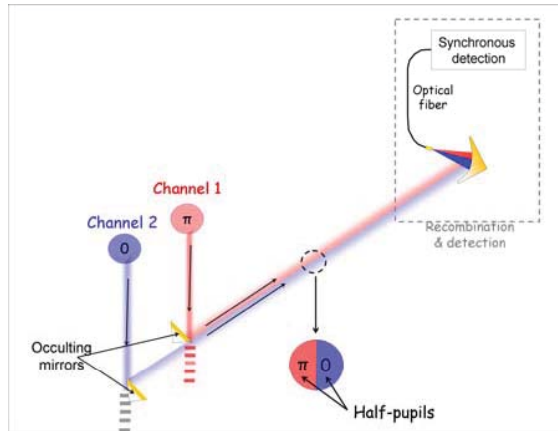


Fig. 5: Multi-axial combination setup on MAII. We use occulting mirrors to reflect half-pupils taken from each arm of the interferometer. An off-axis parabola focuses the composite beam onto the fibre entry.

3. RESULTS

3.1. Double-polarization

In Figure 6 we show a 120 s record for single-polarization nulling versus time at the sampling frequency $f = 200$ Hz.

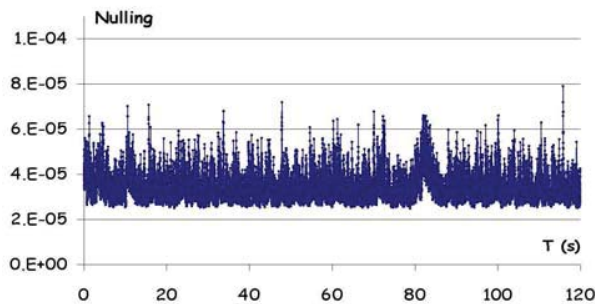


Fig. 6: Double-polarization nulling $N(t)$, polychromatic source ($\lambda_0 \approx 1,55 \mu\text{m}$, $\Delta\lambda/\lambda \approx 5\%$).

Over the interval of 120 seconds, the average value of the nulling is : $\langle N \rangle = 3. \cdot 10^{-5}$ and the standard deviation is : $\sigma_N = 6.10^{-6}$. The best recorded nulling is: $N = 2.7 \cdot 10^{-5}$.

3.2. Single polarization

In Figure 7 we show a record for single-polarization nulling versus time.

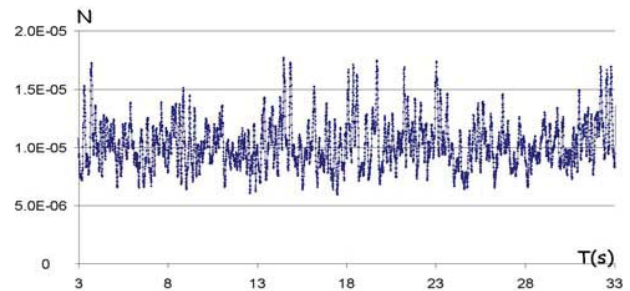


Fig. 7: Single-polarization nulling $N(t)$, polychromatic source ($\lambda_0 \approx 1,55 \mu\text{m}$, $\Delta\lambda/\lambda \approx 5\%$).

Over the interval of 30 seconds, the average value of the nulling is : $\langle N \rangle = 9. \cdot 10^{-6}$ and the standard deviation is : $\sigma_N = 5.10^{-7}$. The best recorded nulling is: $N = 6. \cdot 10^{-6}$. The residual output power is attributed to high frequency OPD integrated during the acquisition time ([2] & [3]).

4. DISCUSSION

4.1. Comparison between MAII and JPL results

Haguenaer & Serabyn validated in 2005 the principle of the multi-axial single mode recombination by using a experimental setup [5] which uses a monochromatic (visible wavelength) and single-polarization source.

Despite the significant differences between the two setups (different spectral domain, different bandwidth, different conditions of polarization), the MAII and JPL results are in the same order of magnitude. Both results confirm the efficiency of the multi-axial combination scheme.

Double-polarization nulling versus single polarization nulling

In 2005, AAS and "Observatoire de la Côte d'Azur" focused their attention on the non-degeneracy of the fundamental modes of an optical fibre used in a nulling interferometer (Buisset & al., SPIE 2006) [6]. A difference between the double-polarization nulling and the single-polarization nulling exists if the fundamentals mode of the optical fibres (involved in the star simulator and the recombination) are not degenerated.

The conclusions of this work are summarized below:

- **Optical fibre with non-degenerated modes:**

The amplitude profile of the fundamental mode is not symmetric. Moreover, this profile is polarization dependant (figure 5) and thus the amplitude mismatch depends with the polarization.

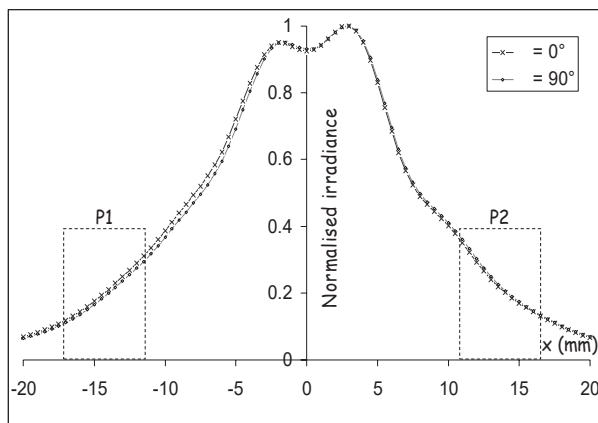


Fig 8: Irradiance profiles, fibre with non-degenerated modes, linear polarization $\theta = 0^\circ$ and $\theta = 90^\circ$. Locations of pupils are also featured.

- **Optical fibre with degenerated modes:**

The profile of the fundamental mode is symmetric and doesn't vary with the polarization. A fibre with degenerated modes preserve the double-polarization nulling.

By taking into account these observations, we made sure that the fibres employed in the star simulator and in the recombination parts of MAII have degenerated modes to prevent from a polarization dependency of the flux mismatch.

The difference double-polarization nulling ratio ($N=3.10^{-5}$) and single-polarization nulling ratio ($N=9.10^{-6}$) is attributed to differential birefringence. Indeed, no compensator of polarization has been set on the bench.

4.2. Stability of the nulling

In the framework of the Darwin & TPF missions, the depth of the nulling is necessary but not sufficient: the stability of the nulling is also crucial.

In the record shown on figure 6, the OPD has been left free to evolve so as to record data in a totally passive mode. Otherwise, the null is stable at $N = 3.10^{-5}$ over a duration of 80 s.

In the record shown figure 7, the OPD has been left free to evolve so as to record data in a totally passive mode. The nulling is stable $N = 9.10^{-6}$ over a duration of 30 s.

We routinely obtain deep nulling ratios stable as in figure 6 and figure 7 over typically one minute with MAII in a laboratory environment. Acoustic noise (transmitted by the atmosphere) and mechanical vibrations are present.

In this context, these results are particularly encouraging.

4.3. Co-axial combination versus multi-axial

The nulling experiments with MAII allow a comparison to be made between the co-axial and the multi-axial combination schemes.

We use 2 kinds of IOBC for the co-axial combination in MAII: the tricoupler and the Y-junction ([2] & [3]). All the results (tricoupler, Y-junction and multi-axial) are in the same order of magnitude: $N \approx 10^{-5}$.

5. CONCLUSION

The MAII testbed has been upgraded to test the multi-axial single-mode combination in polychromatic single-polarization and double-polarization regimes.

With the multi-axial combination, polychromatic nullings as better as $N = 9.10^{-6}$ (single polarization) and $N = 3.10^{-5}$ (double polarization) have been achieved. When the OPD is left free to evolve, these results are stable over one minute.

We have thus demonstrated that the multi-axial single mode combination is efficient at Darwin & TPF nulling levels in the polychromatic single-polarization and double-polarization cases.

6. ACKNOWLEDGMENT

The PhD grant of C. Buisset is co-funded by Alcatel Alenia Space and Centre National de la Recherche Scientifique. The reported studies are supported by ESA in the framework of the Kongsberg-led "Fibre Optic Wavefront Filtering", by Alcatel Alenia Space and by Observatoire de la Côte d'Azur, Dpt Gemini, UMR CNRS 6203

7. BIBLIOGRAPHY

1. ESA, *Darwin the infrared interferometer*, ESA-SCI 12, 2000.
2. Weber et al., *Nulling interferometer based on an Integrated Optic Beam Combiner*, Proc. SPIE 5491, Glasgow, 2004.
3. Barillot et al., *MAI² nulling breadboard based on integrated optics: test results*, Proc. ICSO, 2004.
4. Wallner et al., "Multi-axial single-mode combiner", Proc. SPIE 5491, 798-805, 2004.
5. Haguenaer & Serabyn, *Deep nulling of laser light with a single-mode-fibre beam combiner*, Applied Optic Vol. 45, N° 12, 20 April 2006.
6. Buisset et al., *Multi-axial interferometry: demonstration of deep nulling and investigation of polarization effects*, Proc. SPIE, Orlando, 2006 (to be published).